Antiferritin Single-Chain Fv Fragment Is a Functional Protein with Properties of a Partially Structured State: Comparison with the Completely Folded V_L Domain†

Sergey P. Martsev,*,‡ Alexander A. Chumanevich,‡ Alexander P. Vlasov,‡ Anatoly P. Dubnovitsky,‡ Yaroslav I. Tsybovsky,‡ Sergey M. Deyev,§ Anna Cozzi,|| Paolo Arosio,||,⊥ and Zinaida I. Kravchuk‡

Institute of Bio-Organic Chemistry, Minsk 220141, Belarus, DIBIT, Scientific Institute H. San Raffaele, Milano, Italy, Cattedra di Chimica, University of Brescia, Brescia, Italy, and Engelhardt Institute of Molecular Biology and Institute of Gene Biology, Moscow, Russia

Received August 31, 1999; Revised Manuscript Received February 2, 2000

ABSTRACT: Differential scanning calorimetry and spectroscopic probes were applied to study folding and stability of the single-chain Fv fragment (scFv) of the anti-human ferritin antibody F11 and its isolated variable light-chain (V_L) domain. The scFv fragment followed variable heavy-chain domain (V_H)−linker−V_L orientation and contained $(Gly_4Ser)_3$ linker peptide. The two proteins were produced in *Escherichia coli* and refolded from denaturant-solubilized inclusion bodies. The isolated V_L domain demonstrated a typical immunoglobulin fold with well-defined secondary and tertiary structure and was capable of binding human ferritin with $K_a = 1.8 \times 10^7$ M^{-1}, $\sim 1/30$ of the affinity of the parent F11 antibody. Involvement of this V_L domain into the two-domain scFv fragment yielded a distorted secondary and significantly destabilized tertiary structure in which neither of the two constituent domains attained complete folding. The thermal unfolding enthalpy of scFv F11 at pH 7.0 was as low as 5.0 $J \cdot g^{-1}$ versus 16.3 $J \cdot g^{-1}$ obtained for the V_L domain and 24.7 $J \cdot g^{-1}$ for the parent F11 antibody (mouse IgG2a subclass). Intrinsic fluorescence and near-ultraviolet circular dichroic (CD) spectra, and binding of the hydrophobic probe 8-anilino-1-naphthalene sulfonate, confirmed partial loss of tertiary interactions in scFv. The spectroscopic and calorimetric properties of scFv F11 under physiological conditions are consistent with a model of a partially structured state with a distorted β-sheet as a secondary structure and partial loss of tertiary interactions, which closely resembles the alternatively folded A-state adopted by an immunoglobulin at pH 2−3 [Buchner, J., Renner, M., Lilie, H., Hinz, H.-J., Jaenicke, R., Kiefhaber, T., and Rudolph, R. (1991) *Biochemistry 30*, 6922−6929]. However, scFv F11 demonstrated only an ∼4-fold decrease in the antigen-binding affinity ($K_a = 1.3 \times 10^8$ M^{-1}) versus the parent F11 antibody. The scFv fragment F11 provides the first description of a functional protein trapped under physiological conditions in a partially structured state. This state is either close to the native one in the antigen-binding affinity or, alternatively, initial weak binding of the antigenic epitope induces folding of scFv F11 into a more structured conformation that generates relatively high affinity.

Single-chain variable fragments (scFvs)[1] of immunoglobulins, frequently also referred to as single-chain antibodies, were designed as potentially useful means of targeting cytotoxic agents to tumor cells (*1, 2*). In addition, study of recombinant antibody fragments is an important milestone on the way toward establishing mechanisms underlying folding of multidomain proteins. The scFv fragments comprise two immunoglobulin variable domains covalently joined with a flexible linker peptide and follow the V_H−linker−V_L or V_L−linker−V_H orientation. Depending on the length of a linker peptide, antibody sequence, and solvent conditions, scFv fragments can form dimeric, trimeric, and oligomeric species, with a 15-residue linker being optimal for providing the maximal percentage of monomers (*3*−*6*).

An antigen-binding site spans a significant part of a structure in scFv fragments, and therefore CDR loops lining the surface of this binding site may potentially represent an

† This work was supported in part by grants from the Soros Foundation in Belarus (18-96-2020-8), Foundation for Basic Research of the Republic of Belarus (B98-221), and Russian Foundation for Basic Research (99-04-48836). The fellowship of S.P.M. at DIBIT, Scientific Institute H. San Raffaele, Milano, was supported by EMBO Grant ASTF8609, and S.M.D. was supported by grants from Frontiers in Genetics (Russia) and from Swiss National Science Foundation (Grant 7SUPJ48506).

* Corresponding author: tel +375 172 637 188; fax +375 172 637 274; e-mail martsev@ns.iboch.ac.by.

‡ Institute of Bio-Organic Chemistry, Minsk.

§ Engelhardt Institute of Molecular Biology and Institute of Gene Biology, Moscow.

|| DIBIT, Institute H. San Raffaele, Milano.

⊥ Cattedra di Chimica, Brescia.

[1] Abbreviations: ANS, 8-anilino-1-naphthalene sulfonic acid; BSA, bovine serum albumin; CDR, complementarity-determining region(s) lining the surface of an antigen-binding site in immunoglobulin variable domains; C_H1, the first constant domain of an immunoglobulin heavy chain; C_L, the constant domain of an immunoglobulin light chain; DSC, differential scanning calorimetry; DTNB, 5,5′-dithiobis(2-nitrobenzoic acid); ELISA, enzyme-linked immunosorbent assay; IPTG, isopropyl β-D-thiogalactopyranoside; PMSF, phenylmethanesulfonyl fluoride; scFv, V_L, and V_H, single-chain variable Fv fragment and variable light-, and heavy-chain domains of an immunoglobulin molecule; ΔC_p, heat capacity change between native and termally unfolded states of a protein; Δh, specific calorimetric enthalpy of unfolding; ΔH, molar calorimetric enthalpy of unfolding; T_m, midpoint temperature of thermal transition; $T_{1/2}$, half-width of thermal transition of a protein.

10.1021/bi992036d CCC: $19.00
Published on Web 06/16/2000

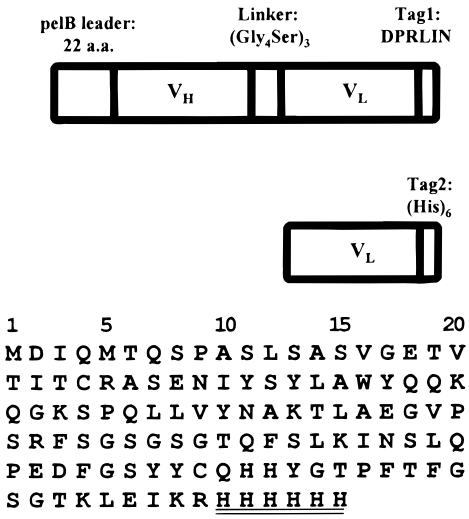

FIGURE 1: Schematic diagram of the expression units for the scFv fragment F11 and its isolated V_L domain, and the amino acid sequence of the V_L domain. Underlined is the $(His)_6$ tag added to the C-terminus of the V_L domain. The sequence of the scFv fragment F11 was reported in ref *19*.

essential determinant of folding and stability of single-chain antibodies. Structural energetics of scFvs as a reliable and quantitative measure of their folding and stability was not determined by the high-resolution method of differential scanning calorimetry because of a pronounced protein aggregation that might occur below an unfolding temperature (*7*, *8*). In the only calorimetric study of scFv recently reported (*9*), the heat capacity profile was incomplete because of the aggregation process observed a few degrees above the midpoint temperature, which precluded thermodynamic measurements. However, stability measurements using denaturant-induced unfolding curves were performed for many scFv fragments and revealed significant variations between them (*7*, *10*−*13*). Differences in CDR loops resulted in significant effects on thermal stability of noncovalently linked Fv fragments (V_H−V_L heterodimers) of the anti-lysozyme antibody D1.3 (*14*). Furthermore, CDR loops were reported to significantly contribute to stability of recombinant human V_L domains (*15*−*17*). Some mutations in CDRs resulted in a dramatic decrease in V_L stability and tertiary interactions as demonstrated by fluorescence and CD spectroscopy. On the other hand, noncognate domain interactions in a cyclic "head-to-tail" trimer of scFv (the so-called "triabody") were shown to alter tertiary interactions of the V_H CDR3 loop involved in the antigen binding site and V_H−V_L domain interface (*18*).

Recently, we reported construction of the anti-human ferritin scFv fragment F11 that was produced in *Escherichia coli* inclusion bodies and refolded from the denaturant to a functional conformation (*19*). We employed the V_H−linker−V_L orientation (Figure 1), starting with the N-terminal V_H domain and the most frequently used $(Gly_4Ser)_3$ linker that provides sufficient flexibility and hydrophilicity (*1*, *5*). The parent F11 antibody (mouse IgG2a subclass) is directed against a tumor marker, human ferritin (*20*, *21*). The two distinctive features of the parent antibody F11 are (i) a significantly lower enthalpy of thermal unfolding in comparison with the other anti-ferritin monoclonals of IgG2a and IgG1 subclasses and (ii) unusual interactions between the antigen-binding domains and the Fc fragment as demonstrated by negative cooperativity between the antigen and protein A binding sites (*21*). These two features were attributable to the structure of CDR loops. Here, we applied the differential scanning calorimetry and spectroscopic probes to analyze folding and stability of the scFv F11 in comparison with the isolated V_L domain of the same antibody fragment. We showed that the isolated V_L domain demonstrates apparently complete folding into a well-defined tertiary structure with moderately low binding affinity. In contrast to V_L, the scFv fragment F11 under physiological conditions adopted a partially structured conformation that is, however, capable of binding antigen and generating relatively high affinity; this combination of properties has not been reported so far.

MATERIALS AND METHODS

Reagents and Enzymes. The employed reagents and enzymes for recombinant DNA technique, as well as standard bacterial strains and plasmids, were described in our recent publication (*19*).

ScFv-Encoding Plasmid and scFv Fragment F11. Construction of the pETscF11 plasmid, expression, purification, and refolding of scFv F11 into soluble conformation was recently described (*19*). The scFv fragment was about 98% pure as judged by SDS−PAGE.

Construction of V_L-Expressing pETVL Plasmid. The V_L domain-encoding plasmid pETVL (Figure 1) was generated by standard techniques from the pETscF11 plasmid that encodes the antiferritin scFv fragment F11 comprising the V_H domain followed by the linker peptide and the V_L domain. Briefly, the V_L-encoding fragment was amplified by PCR from pETscF11 DNA with a direct primer (5′-GCCGCCCATATGGACATCCAGATGACTCAGTCT-3′) comprising the *Nde*I restriction site and a reverse primer (5′-GCCGCCGGATCCCTAGTGGTGGTGGTGGTGGTGCCGTTTTATTTCCAACTTTGT-3′) to insert a *Bam*HI restriction site and to add a six-histidine tag to the C-terminus of V_L. The resulting V_L gene was digested with *Nde*I and *Bam*HI and ligated into the *Nde*I/*Bam*HI-digested plasmid pET12b under a control of T7 RNA polymerase promoter. A ligation mixture was used to transform *E. coli* BL21(DE3)-pLysS cells. The resulting construct pETVL comprised the sequence encoding the V_L domain, starting with additional N-terminal Met. Following the sequence encoding the C-terminal Arg that belongs to the native C-terminus of the V_L domain in the full-length F11 antibody, the recombinant V_L domain comprised the C-terminal $(His)_6$ tag added to permit affinity purification by immobilized metal affinity chromatorgaphy (IMAC) on Ni−NTA Sepharose for crystallization studies. Instead of His hexapeptide, the scFv fragment F11 comprised the C-terminal sequence Asp-Pro-Arg-Leu-Ile-Asn that contains an acid-labile Asp-Pro bond introduced for further designing cleavable fusion constructs.

Expression of the V_L Domain. E. coli BL21(DE3)pLysS cells transformed with the pETVL plasmid were grown in 1 L of LB broth containing ampicillin (100 mg L^{-1}) and chloramphenicol (170 mg L^{-1}) at 37 °C until the culture reached mid-log phase. After 2.5−3.0 h of growth, isopropyl β-D-thiogalactopyranoside (IPTG) was added to a final concentration of 1 mM and the bacterial cells were grown for additional 3 h at 30 °C. The cells were harvested by

centrifugation at 3000*g* for 10 min and washed twice with 150−200 mL of 50 mM Tris-HCl, pH 8.0, containing 0.15 M NaCl and 1 mM phenylmethanesulfonyl fluoride (PMSF). The cells were resuspended in 60−80 mL of the above buffer, disintegrated by sonication, and centrifuged at 40000*g* for 30 min. The sediment of inclusion bodies typically contained V_L domain of 70−80% purity.

Purification of the V_L Domain. The pellet of inclusion bodies containing V_L domain was solubilized with 6 M GdnHCl for 1 h at room temperature. After centrifugation for 30 min at 40000*g*, the supernatant was dialyzed against 5 M urea in 0.1 M Tris-HCl buffer, pH 8.0, with 1 mM PMSF and then centrifuged to remove precipitated material and dialyzed against 1 M urea in 0.1 M Tris-HCl buffer, pH 8.0, with 1 mM PMSF. The supernatant after centrifugation for 30 min at 40000*g* was stored at −20 °C up to 12 months. To refold the protein, supernatant was dialyzed against 50 mM sodium phosphate, pH 7.4, containing 1 mM PMSF. Typically, the yield of the purified and refolded V_L domain was 40−60 mg/L of the cell culture.

Human Spleen Ferritin and Parent F11 Antibody. Human spleen ferritin was isolated as previously described (*20*, *22*). The parent monoclonal antiferritin antibody (IgG2a/κ) produced by the F11 hybridoma cell line and previously described as the antibody HSF102 (*20*, *21*) was purified from ascitic fluid by the procedure of McKiney and Parkinson (*23*). To obtain biotinylated F11 antibody, 0.36 mg of biotin amidocaproate *N*-hydroxysuccinimide ester dissolved in 0.12 mL of dimethyl formamide to give a reagent-to-protein molar ratio of approximately 120:1 was added to 1.0 mL of protein solution containing 1.0 mg of F11 antibody. After 3 h, the antibody solution was dialyzed against 0.1 M sodium borate buffer, pH 8.5.

Antigen-binding affinity was determined by a competition enzyme-linked immunosorbent assay (ELISA) at room temperature in triplicate as we previously described (*19*). Variations of K_a determinations were within 25%. The procedure comprised competition of the scFv fragment or V_L domain with the parent biotinylated antibody F11 for binding to ferritin adsorbed onto a surface of polystyrene tubes.

Enzyme Immunoassay for scFv. The scFv fragment in amounts as low as 0.2−200 ng was determined in a two-site immunoassay performed at room temperature in triplicate with variations of individual measurements below 6%. Polystyrene tubes were coated with 3 μg of rabbit anti-scFv IgG obtained from antisera of rabbits immunized with the scFv fragment F11. The unbound protein was removed by aspirating and washing three times with the coating buffer (0.1 M sodium borate, pH 8.5). Residual protein binding sites on the polystyrene surface were then blocked for 40 min with 1% BSA in 0.1 M sodium phosphate, pH 7.4. Into each tube was introduced 250 μL of a solution containing variable amounts of scFv. After 2 h, the tubes were washed twice with distilled water, 250 ng of biotin conjugated with anti-scFv rabbit IgG was added, and the samples were incubated for 1.5 h. After two washings with distilled water, 250 ng of streptavidin−horseradish peroxidase conjugate was introduced into each tube; they were then incubated for 40 min and washed twice as above. Bound peroxidase activity was determined by adding 0.6 mL of the substrate solution containing 0.02 M *o*-phenylenediamine and 0.02 M H_2O_2 in 0.1 M sodium citrate, pH 5.0. After 10 min with shaking, the reaction was stopped with 0.3 mL of 10% H_2SO_4, and the absorbance was determined at 492 nm. The amount of scFv in samples was calculated from a calibration curve that was obtained with the known amount of scFv (0.2−200 ng/tube) determined from molar extinction at 280 nm. Bound peroxidase activity in the tube containing 0.2 ng of scFv was from 8 to 10 times higher than the background activity (in the absence of scFv), which provided a reliable estimate of scFv in samples with stoichiometry as high as 95−98% (see below).

Stoichiometry of scFv. To estimate the stoichiometry of the functional antigen-binding sites, [*n*], a sequential saturation assay was performed at room temperature. Human spleen ferritin was covalently coupled through protein amino groups to polystyrene balls (6.3 mm in diameter) bearing surface-exposed phenaldehyde groups (the product of the Institute of Physical Organic Chemistry, Minsk, Belarus). Typically, 100 balls were incubated with 6 mg of human spleen ferritin in 300 mL of 0.01 M PBS, pH 7.4. After 6−10 h with shaking, balls were placed into a series of polystyrene tubes and residual protein-binding sites on the polystyrene surface were blocked as above. Then, 3 mL of the solution of scFv fragment F11 (0.2 μg·mL^{-1} in the same buffer) was placed into the first tube. After incubation for 1 h with shaking, a 250 μL aliquot of the solution was taken to determine the unbound scFv fraction, and the remaining solution was placed into the next tube. This procedure was repeated five times, and unbound scFv was quantitated by the immunoassay as described above. Ferritin-bound scFv was determined as the difference between the amount of the total and unbound protein, and the magnitude of [n] was determined as a ratio of ferritin-bound scFv and total scFv.

CD spectra were recorded on a J-20 spectropolarimeter (Jasco, Japan) at a protein concentrations of 0.5−0.7 mg·mL^{-1} in a thermostated cuvette holder with a 1 mm quartz cell for the far-UV spectra and a 10 mm cell for the near-UV region. Spectra were usually scanned from 250 to 200 nm or from 300 to 250 nm at a scan speed of 5 nm/min and a time constant of 16 s. The averaged spectra of three scans were corrected for the buffer blank. Mean residue ellipticities were calculated by use of a value of 115 for the mean residue weight.

Fluorescence Measurements. Fluorescence spectra of the proteins and protein−ANS complexes were recorded at room temperature and a protein concentration of 0.1 mg·mL^{-1} in a 1 cm path length cuvette on a SFL-1211 fluorometer (Solar, Belarus) as described in ref *24*. The protein tryptophan fluorescence was excited at 295 nm, and the ANS fluorescence was excited at 360 nm. The ANS-to-protein molar ratios were equal to 10, 20, and 120 for the V_L domain, scFv fragment, and parent F11 antibody, respectively, corresponding approximately to the ratio of 10 mol of ANS/mol of antibody domain.

Differential Scanning Calorimetry. Measurements were performed with a DASM-4 scanning calorimeter (Biopribor, Pushchino, Russia) in the temperature range 10−100 °C at a scan speed of 60 K/h. In all experiments the reference cell was filled with the buffer used to dialyze the protein sample. Unless otherwise specified, the buffers used for the calorimetric measurements were as follows: at pH 2.0, 0.05 M sodium phosphate−hydrochloride; at pH 3.0, 0.05 M phos-

phate−citrate buffer; and at pH 5.0 and 7.0, 0.05 M sodium phosphate. From the obtained heat capacity curves, the instrumental baseline was subtracted. The latter was determined prior to each protein scan with both cells filled with the buffer. The protein concentrations in calorimetric experiments ranged between 1 and 2.5 mg·mL^{-1}. Three to four scans were recorded for each sample, with variations of enthalpy measurements being within the range of 5−7% for the V_L domain and parent F11 antibody, and within 10% for the scFv fragment, which had significantly lower transition enthalpy and solubility at high protein concentrations. Calorimetric enthalpy was calculated according to Privalov and Khechinashvili (*25*). Heat capacity curves were analyzed and deconvoluted with software TERMCALC based on the method described by Privalov and Potekhin (*26*). The TERMCALC software was supplied by the DASM-4 manufacturer. The heat capacity function of fully unfolded proteins was calculated according to Makhatadze and Privalov (*27*).

Size-Exclusion Chromatography. The protein oligomerization state was determined by size-exclusion chromatography on a TSK-55f column (0.8 × 50 cm) at room temperature, which was calibrated with molecular mass standards (IgG, 150 kDa; BSA, 67 kDa; ovalbumin, 45 kDa; chymotrypsinogen, 25 kDa). The sample volume was 0.5 mL.

Quantitative Analysis of Disulfides and Free Thiols. The number of disulfides in the purified and refolded proteins, V_L and scFv, was determined by the method of Thannhauser et al. *(28*) in a protein solution containing 3 M GdnSCN, a denaturing agent that does not interfere with the assay. Free thiols were assayed with DTNB as described by Ellman (*29*) both in the presence and absence of the denaturant.

Other Methods. SDS−PAGE was performed according to Laemmli (*30*) and stained with Coomassie Brilliant Blue R-250. Native electrophoresis in the absence of SDS was carried out in a 10% polyacrylamide running gel without a stacking gel. The isoelectric points for the V_L domain and scFv fragment are above pH 8.5, and therefore the standard buffer system with pH 8.8−8.9 in the running gel cannot be applied. The following buffers were used: 0.35% acetic acid−NaOH, pH 5.9, for the running gel; 0.035 M β-alanine, titrated with acetic acid to pH 4.5, as the upper (positive) electrode buffer; and 0.1 M sodium acetate, pH 4.9, as the lower electrode buffer. Concentration of antibodies were determined from the absorption of 0.1% solution in a 1 cm path length cuvette at 280 nm. The absorption values 1.81 for scFv, 1.62 for F11, and 1.12 for V_L were calculated from the known amino acid sequences according to ref *31*.

RESULTS

Purity and Stoichiometry. Each of the two recombinant proteins, V_L and scFv F11, demonstrated a single polypeptide band on SDS−PAGE with apparent molecular masses of 14 ± 1 kDa for V_L and 27 ± 2 kDa for scFv. Previously, two conformers were obtained after refolding of the immunoglobulin light chain comprising V_L and C_L domains (*32*). Given these data, we extended the analysis of purity to consider a hypothesis that our scFv fragment may represent a mixture of two or more refolding conformers, only one of which is functional and completely folded. We obtained at least four lines of evidence that argue against this hypothesis.

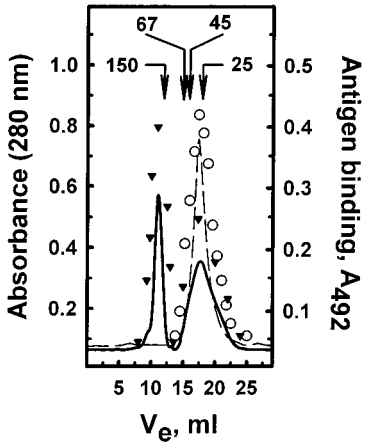

FIGURE 2: Size-exclusion chromatography of the scFv fragment on a TSK-55f column (0.8 × 50 cm) immediately after refolding in 0.1 M phosphate buffer, pH 7.4, and concentrating 8-fold during 8 h (− − −) and after 2 weeks of storage at 2−4 °C (—). Protein concentration: 1.0 mg mL^{-1}. Functional activity, shown for (○) freshly refolded scFv and (▼) scFv after storage, was determined by a competition ELISA (see Materials and Methods). Molecular mass standards: 150 kDa, rabbit immunoglobulin G; 67 kDa, bovine serum albumin; 45 kDa, ovalbumin; 25 kDa, chymotrypsinogen.

First, a single band observed in SDS−PAGE without β-mercaptoethanol for both V_L and scFv (data not shown) suggests the absence of refolding conformers resulting from nonnative disulfide bonding. Second, the separation in PAGE without SDS (not shown) revealed a single band of scFv, thus indicating the lack of other folding conformers. The resolution power of this method was demonstrated by clear-cut separation of the full-length parent antibody F11 and its truncated two- and single-domain versions, scFv and V_L. As a third line of evidence, we failed to isolate any inactive polypeptide(s) from our scFv samples by size-exclusion chromatography (Figure 2). Finally, the stoichiometry of the active antigen-binding sites, [*n*], ranged from 0.93 to 0.98 for different scFv samples. This stoichiometry indicates that scFv F11 purified to electrophoretic homogeneity may contain only a minor amount of a nonfunctional protein. Together, these results strongly suggest that our purification/refolding protocol yielded a single molecular form of scFv rather than two or more refolding conformers.

Monomeric and Multimeric Forms of scFv. Size-exclusion chromatography revealed that fresh samples of the scFv fragment F11 comprised only monomeric species, with higher oligomers (molecular mass exceeding 150 kDa) observed after storage (Figure 2). As demonstrated by the functional assay, these two forms of scFv possessed virtually identical antigen-binding activity. The oligomerization propensity of our scFv is consistent with that reported for several scFv fragments (see refs *31*−*33* as the examples). In previous studies, the propensity of scFvs to produce dimers and trimers was minimal with 15-residue linker peptides, while shorter linkers (from 0 to 10 amino acids) produced mainly dimeric and/or trimeric species (*5*, *6*). Recently, Arndt et al. (*6*) provided convincing evidence that refolding of scFv fragments from denaturant-solubilized inclusion bodies in dilute solutions normally results in predominantly monomeric species, at least in the case of 15-residue linkers and V_H−linker−V_L orientation of scFv, which is fully consistent with our conditions and results. Given oligomerization of a

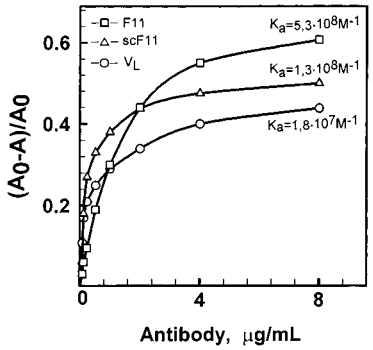

FIGURE 3: Antigen-binding affinity of the scFv fragment and V_L domain determined by competitive ELISA. The K_a values were obtained from double-reciprocal plots.

significant fraction of scFv after 2 weeks of storage (Figure 2), we used freshly prepared monomeric samples (normally stored 3 days or less at 2−4 °C) for spectroscopic and calorimetric measurements.

The V_L domain was found to be a dimer, as judged by size-exclusion chromatography (data not shown), consistent with the well-known tendency of V_L to form dimeric species (see *17*, for a review).

Antigen-Binding Affinity. We found that the V_L domain is capable of antigen binding with an affinity constant of about 1.8×10^7 M^{-1}, ~30 times lower than the affinity of the parent F11 antibody (Figure 3). Previously, a V_H domain was suggested to make a major contribution to generating an antigen-binding site (*36, 37*). However, antigen-binding activity was also reported for the mouse light chain comprising V_L and C_L domains (*32*). For the scFv fragment F11, the affinity constant was only ~4 times lower than that for the parent F11 antibody. Higher affinity of scFv versus the V_L domain suggests that CDR loops of the V_H domain of this antiferritin antibody significantly contribute to generating the antigen binding site.

CD Spectra. The far-UV CD spectrum of the V_L domain (Figure 4A) displayed a negative maximum of mean residue ellipticity at 218 nm in the far-UV region, which is typical for the β-sheet secondary structure of native immunoglobulins. Furthermore, the negative maximum around 280 nm in the near-UV CD spectra (Figure 4B) suggests asymmetric environment of aromatic residues, i.e., the presence of a tertiary structure. Close similarity of CD spectra for parent F11 and V_L (Figure 4A) indicates that the secondary structure of the V_L domain is close or identical to that of parent F11.

In contrast to the V_L domain, the scFv fragment demonstrated a negative ellipticity maximum in the far-UV CD spectrum (Figure 4A), which was 3−4-fold higher than that observed for V_L and full-length parent antibody F11. In addition, the far-UV CD spectrum was distinctly different from a spectrum of the denatured scFv and V_L. These results indicate that the scFv fragment F11 possesses significant amount of β-sheet secondary structure, which is, however, significantly distorted and differs from the structure of both native and denatured immunoglobulin domains. It is noteworthy that a significant (2−3-fold) increase in the negative ellipticity is characteristic for a partially structured state obtained at pH 2−3 for the mouse IgG1 antibody and its Fab fragment (*16, 38, 40*) and for our parent F11 antibody (not shown). The near-UV CD spectrum of scFv F11 in comparison with that of the V_L domain did not display a negative maximum around 280 nm, thus indicating that aromatic residues of scFv lost their asymmetric environment due to the partial loss of tertiary interactions.

Fluorescence Spectra. The intrinsic fluorescence spectrum of the V_L domain (Figure 5) suggests a compact conformation with aromatic fluorophores protected from quenching by solvent, as judged by the emission maximum around 337 nm in the native protein and a red shift to 352 nm observed after unfolding in the denaturant. Furthermore, enhanced emission intensity ("dequenching" effect) was observed after denaturant-induced unfolding, which suggests that aromatic fluorophores in the compact protein are in close proximity with internal quencher generally assigned to the disulfide bond present in immunoglobulin domains (*16, 38, 40*). Together, CD spectra and "dequenching" effects observed for the V_L domain are indicative of the presence of the so-called immunoglobulin fold that is characteristic for native immunoglobulins.

Similarly to the V_L domain, scFv demonstrated a fluorescence emission maximum at 337 nm and a red shift in the emission wavelength after addition of the denaturant (Figure 5), suggesting a compact conformation of the scFv fragment with aromatic residues involved in a hydrophobic core. However, scFv did not display "dequenching" after denaturant-induced unfolding, which indicates spatial separation of quencher and aromatic fluorophores. This finding suggests either incomplete or at least nonnative tertiary folding of the scFv fragment F11.

ANS is the generally accepted probe for partially structured states of proteins. This hydrophobic dye does not bind to completely folded native proteins, nor does it interact with unfolded polypeptides. However, fluctuating tertiary structure of partially unfolded states allows the access of ANS to a protein hydrophobic core hidden in the native state or lost in unfolded polypeptides (*41, 42*). Our ANS-binding studies demonstrate that neither native nor denaturant-unfolded states of the V_L domain bind the hydrophobic dye (Figure 6). In contrast, scFv F11 under physiological conditions demonstrates pronounced binding of ANS, which is indicative of a partially unfolded tertiary structure. Our observation that the V_L domain at pH 7 does not bind ANS indicates that high ANS binding propensity observed for scFv F11 cannot be explained by the exposure to solvent of the V_L and V_H domain interfaces that are hidden in the native immunoglobulins by the partner C_L and C_H1 domains.

Differential Scanning Calorimetry. Thermodynamic stability of the parent antibody F11 and its recombinant fragments, scFv and the V_L domain, was compared in terms of specific transition enthalpies, Δh, calculated per gram of protein in order to disregard differences in their molecular mass. In repetitive cycles of heating and cooling of protein samples in the calorimetric cell, thermal unfolding of the three proteins revealed variable degrees of reversibility depending on the protein, pH, and the end temperature of the first scan. Although thermodynamic measurements are formally allowed for processes that possess reversibility of a thermal transition (*25, 43*), it was more recently shown that the quantitative calorimetric analysis is admissible also for transitions having little or no reversibility (*44*−*46*). Major arguments were attributed to the findings that the irreversible part of the process (i.e., thermal aggregation at near-transition temperatures, in most cases) is generally slow and does not

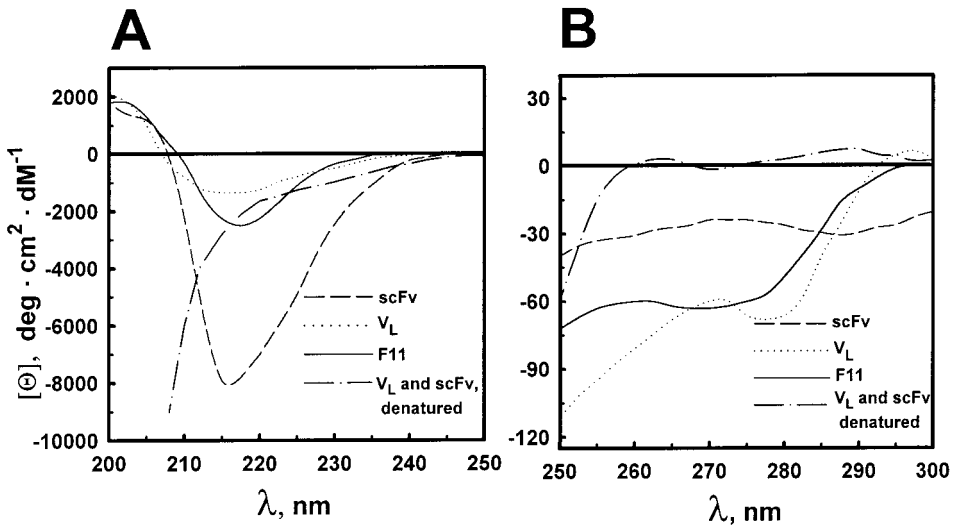

FIGURE 4: Far-UV (A) and near-UV (B) CD spectra of the scFv fragment, V_L domain, and parent monoclonal antibody F11. For the unfolded scFv fragment and V_L domain (4.5 M GdnHCl), the two curves coincide.

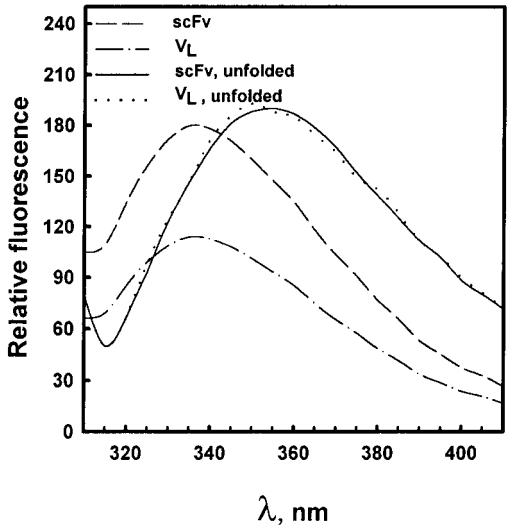

FIGURE 5: Fluorescence spectra of the scFv fragment, V_L domain, and parent F11 antibody. Protein concentration: 0.1 mg mL^{-1}. Buffer: 0.05 M sodium phosphate, pH 7.

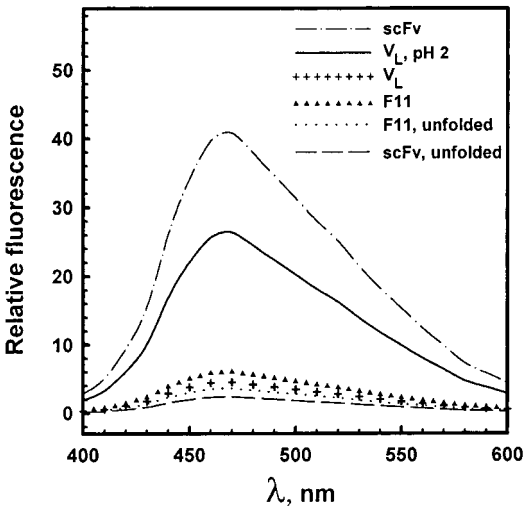

FIGURE 6: Binding of a hydrophobic probe, 8-anilino-1-naphthalene sulfonate (ANS), to the scFv fragment, V_L domain, and parent F11 antibody.

interfere with calorimetric measurements. Differential scanning calorimetry of the V_L domain (Figure 7A,B) revealed a highly cooperative thermal transition between pH 3 and 7, with a high degree of reversibility at acidic pH. At pH 7.0 (Figure 7B), a sharp peak of thermal unfolding with the half-width $T_{1/2} = 6$ °C, was obtained at the midpoint temperature $T_m = 60.5$ °C. The specific calorimetric enthalpy of thermal unfolding was about 16.3 $J \cdot g^{-1}$, which is close to the values obtained for many fully compact proteins with well-defined tertiary structure. For the parent antibody F11, the transition enthalpy at pH 7 was significantly higher (24.7 $J \cdot g^{-1}$), which may indicate significant contribution of domain interactions to stability of the naturally occurring immunoglobulins.

Dramatic differences in the heat capacity functions were observed for the scFv fragment in comparison with the V_L domain and parent F11 (Figure 7A,B). Thermal unfolding of scFv at pH 7.0 did not display a sharp heat absorption peak. Instead, calorimetry revealed a broad low-cooperative transition with a small enthalpy, 5.0 $J \cdot g^{-1}$; this transition was irreversible. In the pretransition region, the specific heat capacity of the scFv was intermediate: it exceeded the heat capacity of the native V_L domain (Figure 7B) and parent antibody (Figure 7A) but did not reach the value obtained for the denatured states, as demonstrated by the second scan. This finding indicates partial exposure of hydrophobic amino acids in scFv F11, consistent with the prominent ANS-binding capacity shown for this protein. It is noteworthy that the midpoint of thermal transition of scFv F11 is unexpectedly high ($T_m = 57$ °C) when compared to the T_m of the destabilized states of V_L and parent F11 obtained at pH 3 (40 and 49 °C, respectively). This combination of remarkably low Δh and high T_m is characteristic of a partially structured state of an immunoglobulin, the so-called alternatively folded state (*38*). Together, our calorimetric data strongly suggest a partially structured conformation of the scFv fragment F11 at pH 7.0.

The ratio of the calorimeric-to-van't Hoff enthalpies (the cooperativity ratio, CR) obtained for the scFv fragment was close to unity and varied between CR = 0.93 and 1.12 for different scFv preparations, which is suggestive of a two-state unfolding of a single calorimetrically revealed folding unit. Accordingly, quantitative deconvolution of the heat capacity curve of scFv F11 yielded a single all-or-none

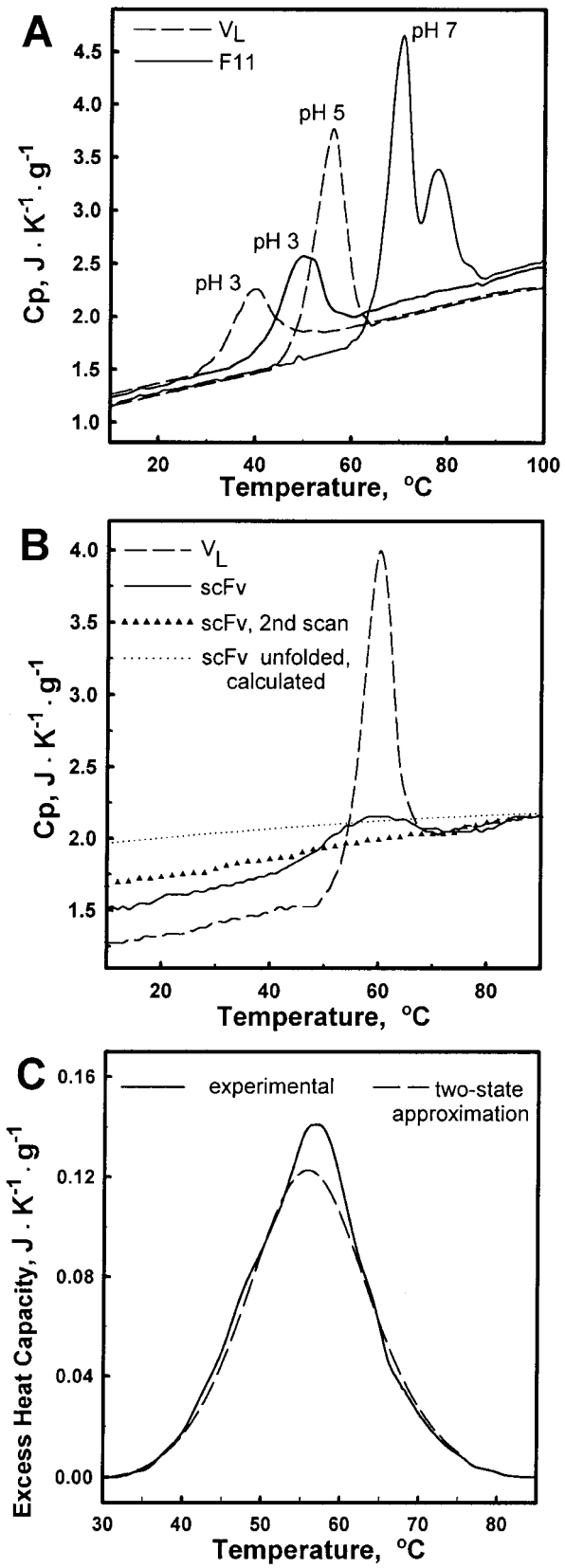

FIGURE 7: Differential scanning calorimetry of the scFv fragment and V_L domain in comparison with the parent F11 antibody. Panels A and B: Heat capacity functions obtained at pH 3, 5, and 7 (A) and at pH 7 (B). Panel C: Deconvolution analysis of the excess heat capacity function of the scFv fragment. The dotted curve in panel B shows the predicted heat capacity profile for the unfolded scFv fragment, which was calculated according to Makhatadze and Privalov (*27*). The buffers used were, at pH 7.0 and 5.0, 0.05 M sodium phosphate, and at pH 3.0, 0.05 M sodium phosphate−citrate.

thermal transition (Figure 7C). It is noteworthy that the V_L domain comprises ~50% of the molecular mass of our scFv, while the specific transition enthalpy of scFv was only ~30% of that determined for the V_L domain. Therefore, the low transition enthalpy of scFv F11 cannot be attributed to a "bipartite" structure (as reviewed in ref *47*) comprising completely folded V_L and unfolded V_H domain. Significant contribution of the V_H domain to generating the antigen-binding site (Figure 3) also argues against this hypothesis. Thus, from our calorimetric and functional studies we have no choice but to conclude that both V_L and V_H domains in the scFv fragment F11 adopt a partially structured conformation.

Disulfide Bonds and Free Thiols. Determination of the number of disulfides under denaturing conditions for five different scFv samples gave a mean value of 1.94 mol/mol of scFv (variation range: 1.87−2.04 mol of disulfides/mol of scFv). This result is fully consistent with four Cys residues generally present in scFv fragments and one disulfide bond per each V_H and V_L domain. The maximal content of free thiols determined by Ellman's method (*29*) was 0.15 mol/mol of scFv, which is less than 4% of the molar amount of Cys residues in the scFv fragment. These results demonstrate that our scFv fragment does not comprise free thiols, stable oxygen derivatives of Cys residues, or presumed mixed disulfides with cellular mercaptans in appreciable amounts that would provide an alternative explanation for incomplete folding of scFv through incorrectly or incompletely bonded disulfides.

For the V_L domain, the maximal number of free thiols was ~3% of the molar amount of Cys residues. The mean value for the number of disulfides estimated under denaturing conditions was 0.96 mol/mol of V_L (variation range for four different samples: 0.93−1.02 mol of disulfide/mol of V_L). Virtually identical content of disulfides and free thiols determined for the scFv fragment and V_L domain is not surprising as long as the two proteins passed through a similar purification/refolding procedure under nonreducing conditions in the presence of oxygen. Although this procedure does not seem to provide as high potential of forming correct disulfides as a series of specially designed methods (e.g., see refs *48*−*50*), it appeared efficient enough in forming correctly folded and functional V_L domain. In addition to the lack of refolding conformers and a stoichiometry of disulfides and thiols, complete folding of the V_L domain provides a further indication that argues against involvement of incomplete or incorrect disulfide bonding in formation of a partially structured state of the scFv fragment F11.

DISCUSSION

In this study, we analyzed folding of the isolated V_L domain of the full-length F11 antibody in comparison with the scFv fragment F11 that involves the V_L and V_H domains in the V_H−linker−V_L orientation. The isolated V_L domain is a homodimer and possesses apparently native secondary and tertiary structures that adopt a typical immunoglobulin fold, as demonstrated by CD and fluorescence spectra and differential scanning calorimetry. Stability of the tertiary structure in terms of the thermal transition enthalpy is consistent with stability of fully compact proteins. The V_L domain is capable of binding to the antigen with moderately

low affinity ($K_a = 1.8 \times 10^7$ M^{-1}), approximately $^1/_{30}$ that of the full-length parent antibody F11.

In contrast to apparently complete folding of the isolated V_L domain, its coupling to the partner V_H domain via nonnative linker peptide produces the protein in which neither V_L nor V_H domain attains complete folding into a well-defined tertiary structure. The secondary structure of the scFv fragment F11 can be characterized as a significantly distorted β-sheet, and the tertiary structure demonstrates partial loss of stabilizing interactions. At least three lines of evidence indicate that the scFv fragment F11 under physiological conditions possesses properties of a partially structured intermediate-like state. The first line of evidence was provided by the fluorescence spectra suggesting spatial separation of an internal quencher (presumably the two disulfide bonds) and aromatic residues in scFv. Spatial proximity of aromatic fluorophores and a quencher is a general feature of the native immunoglobulin fold (*16*, *38*, *40*) and was observed both in the parent F11 antibody and in its isolated V_L domain (Figure 5). In addition, a partial loss of tertiary interactions in scFv F11 was confirmed by the loss of asymmetric environment of aromatic residues as demonstrated by near-UV CD spectra (Figure 4B). The most convincing is the second, calorimetric line of evidence indicating that a tertiary structure of scFv F11 is significantly destabilized and undergoes low-cooperative thermal transition with remarkably low unfolding enthalpy ($\Delta h = 5.0$ J·g^{-1} versus 16.3 and 24.7 J·g^{-1} for the V_L domain and parent F11, respectively). The heat capacity of the native state is intermediate between the values observed for the native and unfolded states, which indicates partial exposure of hydrophobic residues hidden in the native protein. This is fully consistent with our third observation that the structure of scFv permits the access for ANS to hydrophobic sites that are not exposed in the native proteins, V_L and the parent F11 antibody. However, partial tertiary interactions remaining in scFv F11 are sufficient to provide stability against a chemical denaturant, as demonstrated by the cooperative unfolding transition (*19*). Furthermore, the scFv fragment F11 is functional, it preserves a hydrophobic core, and it still retains evident, yet greatly reduced, cooperativity of thermal unfolding, which collectively indicates the presence of a tertiary structure in scFv F11.

As an alternative explanation, intermediatelike spectroscopic and calorimetric properties of a functional protein could have been attributed to a mixture of conformational states (*47*) that in our case would comprise both native functional and nonnative nonfunctional conformations. However, given the stoichiometry of functional binding sites in our scFv (from 93% to 98%), the population of the nonfunctional protein is very low and cannot explain a more than 3-fold increase in the negative ellipticity displayed by CD spectrum and a similar decrease in the unfolding enthalpy. Thus, the whole set of calorimetric, spectroscopic, and functional data obtained for scFv F11 cannot be attributed to a presumed mixture of conformational states. Likewise, our measurements of disulfides and free thiols demonstrated that a partially structured state of the scFv fragment F11 cannot result from presumed incomplete formation of disulfide bridges or nonnative derivatives of Cys residues.

The above properties of our scFv remained unchanged when we varied the refolding protocol by changing the number of steps in a sequential dialysis procedure (*19*) or by insertion of additional dialysis at pH 2.0 prior to the final refolding step (not shown). These variations in the refolding/purification protocol resulted in varying the yield, not the properties, of active soluble scFv. This strongly suggests that different refolding conditions yield a single macroscopic state of scFv. This state demonstrates long-term stability for at least several days (*19*) and therefore seems to be trapped in a free energy minimum which is well-separated (presumably by a high activation barrier) from other possible minima. The only source of structural heterogeneity is the appearance of functional oligomeric species during storage, which cannot change our calorimetric and spectroscopic data obtained with monomeric scFv samples.

The changes in CD spectra, together with a high propensity to bind a hydrophobic probe and a combination of the low enthalpy and relatively high transition temperature, demonstrate a remarkable similarity to the corresponding parameters of a partially structured conformation, the so-called alternatively folded state (*A*-state). This state was found at pH 2−3 for the full-length monoclonal antibody MAK33 (mouse IgG1 subclass) and its Fab fragment (*38*, *39*) and confirmed by us for the parent F11 antibody of mouse IgG2a subclass (Vlasov et al., to be published). Formation of this immunoglobulin *A*-state was attributed to nonnative interactions of antibody domains under strongly acidic conditions that induce "reshuffling" of the tertiary and quaternary interactions (*38*). Apocytochrome P-450 is an example of an intermediatelike conformation that is populated under physiological conditions and demonstrates close similarity to our scFv fragment by calorimetric and spectroscopic properties (*51*). The lack of heme or strongly acidic conditions precluded functional studies in the above two examples of partially structured (intermediatelike) states. A series of staphylococcal nuclease mutants provided the first description of engineered proteins significantly unfolded under physiological conditions; these conformations were nonfunctional and attributed to a denatured state with a residual structure (*52*; see ref *53* for a review). Besides the above stable nonfunctional intermediates, a denaturant-induced molten globule-like state of peanut lectin was shown to retain its sugar-binding affinity in 2 M GdnHCl and therefore was reported as a first demonstration of a functional molten globule-like state (*54*). Furthermore, biological activity of proteins involved in membrane translocation processes requires unfolding of a part of their structure in order to penetrate a membrane; therefore, under acidic pH, these proteins usually form partially structured states that are considered as functional (e.g., see refs *55* and *56*).

In this context, the scFv fragment F11 provides an unusual example of a functional partially structured state that, in contrast to previous observations, possesses long-term stability under physiological conditions. The combination of the two apparently contradictive properties, i.e., functionality and partially structured conformation, may be reconciled when considered as an extreme example of known reciprocal relationships between protein stability and functional activity (see refs *57*−*59* for a review; *60*). However, for scFv fragments stability−activity correlation may appear more complicated. It was demonstrated that stability of scFv

proteins and their derivatives can be greatly enhanced, without loss of the binding affinity, through insertion of a disulfide bond in the V_H-V_L domain interface (*61*) or by a more generally applicable approach that involves engineering a disulfide in the conserved framework residues to link the two partner domains (*62*−*66*). The latter approach remained valid for scFv-derived immunotoxins (*67, 68*; see ref *69* for a review). More recently, Warn and Pluckthun (*70, 71*) demonstrated that reinsertion of the naturally lost disulfide bond may provide drastic stabilization of scFv fragments through at least two mechanisms, either increasing intrinsic stability of domains or engineering a more stabile interface.

As an alternative explanation for the unusual combination of conformational and functional properties of the scFv fragment F11, an antigenic epitope of ferritin might induce folding of the scFv fragment F11 into a presumed more structured state that generates moderately high antigen-binding affinity. This assumption involves initial low-affinity binding of the ferritin epitope to a partially disordered conformation and a subsequent conformational transition into a more ordered structure capable of generating higher affinity. The presumed more structured state may possess tighter association between constituent domains and/or their enhanced intrinsic stability. Although this two-step binding mechanism is purely hypothetical and needs experimental verification, apparently a similar mechanism was reported for circularly permuted dihydrofolate reductase (*72*). The mutant reductase possessed all the properties of a molten globule state that, however, underwent a transition to the nativelike conformation after simultaneous binding of the two specific ligands, NADP and inhibitor (methotrexate). When NADPH and the substrate (dihydrofolate) were added, this structure regained functional activity.

Our results indicate that the concept of independent folding of immunoglobulin domains (*73*) is consistent with the properties of the isolated V_L domain but cannot be applied to the two-domain scFv fragment F11. In previous studies, several recombinant V_H domains were described as functional proteins having apparently native conformation (*36, 70, 74*), with few examples of structural resolution by X-ray crystallography or NMR spectroscopy (see ref *75* for a review). Given these data and apparently complete folding of our isolated V_L domain, a partially structured state of the two-domain V_H-linker$-V_L$ construct suggests that a unique structure of CDR loops in the V_H domain or its combination with the linker peptide may contribute to nonnative tertiary and/or quaternary interactions stabilizing the partially structured conformation of the scFv fragment F11. To discriminate between these presumed contributions, additional studies are required that would include the isolated V_H domain and different linkers in our scFv. Recently, Pluckthun and coworkers (*76*−*79*) reported that folding of the anti-phosphorylcholine scFv fragment was characterized by a kinetic trap along the folding pathway that yielded a transiently populated intermediate. In contrast to the scFv fragment, folding of the isolated domains (V_H and V_L) and their noncovalent heterodimer (Fv fragment) devoid of linker peptide did not show such a kinetic trap. Therefore, formation of the partially structured intermediate of the anti-phosphorylcholine scFv fragment was attributed to early interactions of premature conformations of the V_H and V_L domains due to their high local concentration provided by the $(Gly_4Ser)_3$ linker (*79*). From comparison of these (*76*−*79*) and our data, one can speculate that similar underlying forces (i.e., interactions of premature domains) but different values of an energetic barrier between structural states along the folding pathway might result in only transient population of a folding intermediate, as observed for anti-phosphorylcholine scFv fragment, or in long-term stability of the intermediate-like state demonstrated for our scFv fragment F11. Significant contribution of the C-terminal "tag" to folding and stability of the scFv fragment F11 seems unlikely, taking into account both apparently complete folding of our V_L domain bearing the hexapeptide tag and numerous data indicating that a variety of immunoglobulin domains and scFv fragments tolerated variations in C-terminal tags.

Solely on the basis of the present data, it is not possible to decide whether a partially structured conformation is a unique feature of the functional scFv fragment F11 or whether it can also be observed for some other scFv fragments. In the former case, the scFv fragment F11, because of the unusual combination of functional activity, partially structured conformation, and marginal stability may provide a useful experimental system to gain new information on forces underlying folding, stability, and activity of scFv fragments and immunoglobulins. A relatively high propensity of our scFv to form multimeric species and a moderate decrease in the binding affinity versus the parent antibody are consistent with properties reported for many scFv fragments (*11*; see ref *80* for a review). On the other hand, low thermodynamic stability and unique allosteric properties shown for the parent antibody F11 in comparison with the other anti-ferritin monoclonal antibodies of the same IgG2a subclass (*21*) may provide indirect indication in support of a hypothesis that it is the structure of the V_H CDR loops and/or the linker peptide that resulted in the unusual combination of a partially structured state and relatively high affinity of the scFv fragment F11. As another indication in support of this hypothesis, the anti-fluorescein scFv 4-4-20 (*8*) displayed the far-UV CD spectra that suggested an unchanged secondary structure in comparison with the parent antibody (mouse IgG2a). On the contrary, our scFv fragment F11 possesses a significantly distorted secondary structure versus both the full-length F11 antibody and anti-fluorescein scFv 4-4-20, as judged by a comparison of the CD spectra. Finally, although Weber-Bornhauser et al. (*9*) did not obtain complete calorimetric scan of their scFv fragment, our rough estimation of the transition enthalpy from the extrapolated scan gave a value of 16−25 $J \cdot g^{-1}$, which is from 3−5-fold higher than the unfolding enthalpy of our scFv F11 while being close to thermal unfolding enthalpies generally observed for completely folded proteins, including the V_L domain and parent F11 antibody.

ACKNOWLEDGMENT

We are grateful to Dr. Vadim Shmanai for providing us with the activated polystyrene balls and Dr. Sergey Gilevich for helpful suggestions on establishing the disulfide assay.

REFERENCES

1. Bird, R. E., Hardman, K. D., Jacobson, J. W., Johnson, S., Kaufman, B. M., Lee, S.-M., Lee, T., Pope, S. H., Riordan, G. S., and Whitlow, M. (1988) *Science 242*, 423−426.

2. Huston, J. S., Levinson, D., Mudget-Hunter, M., Tai, M.-S., Novotny, J., Margolies, M., Ridge, R. J., Bruccoleri, R. E., Haber, E., Crea, R., and Oppermann, H. (1988) *Proc. Natl. Acad. Sci. U.S.A. 85*, 5879−5893.
3. Whitlow, M., Bell, B. A., Feng, S. L., Filpula, D., Hardmann, K., Hubert, S. L., Rollence, M. L., Wood, J. F., Schott, M. E., Milenic, D. E., Yokota, T., and Scholm, J. (1995) *Protein Eng. 6*, 989−995.
4. Alftan, K., Takkinen, K., Sizmann, D., Soderlund, H., and Teeri, T. (1995) *Protein Eng. 8*, 725−731.
5. Kortt, A., Lah, M., Oddie, G. W., Gruen, C. L., Burns, J. E., Pearce, L. A., Atwell, J. L., McCoy, A. J., Howlett, G. J., Metzger, D. W., Webster, R. G., and Hudson, P. J. (1997) *Protein Eng. 10*, 423−433.
6. Arndt, K. A., Muller, K. M., and Pluckthun, A. (1998) *Biochemistry 37*, 12918−12926.
7. Pantoliano, M. W., Bird, R., Johnson, S., Asel, E. D., Dodd, S. W., Wood, J. F., and Hardman K. D. (1991) *Biochemistry 30*, 10117−10125.
8. Tetin, S. Yu., Mantulin, W. W., Denzin, L. K., Weinder, K. M., and Voss, E. W. (1992) *Biochemistry 31*, 12029−12034.
9. Weber-Bornhauser, S., Eggenberger, J., Jelesarov, I., Bernard, A., Berger, C., and Bosshard, H. R. (1998) *Biochemistry 37*, 13011−13020.
10. Bedzik, W. D., Weidner, K. M., Denzin, L. K., Johnson, L. S., Hardman, K. D., Pantoliano, M. W., Asel, E. D., and Voss, E. D. (1990) *J. Biol. Chem. 265*, 18615−18620.
11. Pluckthun A. (1993) in *Stability and Stabilization of Enzymes*, Proceedings of the International Symposium, Maastricht, The Netherlands, 22−25 November, 1992, pp 81−90, Elsevier Science Publishers BV, Amsterdam.
12. Knappik, A, and Plucktun, A. (1995) *Protein Eng. 8*, 81−89.
13. Nieba, L., Honneger, A., Krebber, C., and Pluckthun, A. (1997) *Protein Eng. 10*, 435−444.
14. Yasui, H., Ito, W., and Kurosawa, Y. (1994) *FEBS Lett. 353*, 143−146.
15. Hurle, M. R., Helms, L., Li, L., and Wetzel, R. (1994) *Proc. Natl. Acad. Sci. U.S.A. 91*, 5446−5450.
16. Helms, L., and Wetzel, R. (1995) *Protein Sci. 4*, 2073−2081.
17. Raffen, R., Stevens, P. W., Boogaard, C., Schiffer, M., and Stevens, F. (1998) *Protein Eng. 11*, 303−309.
18. Pei X. Y., Holliger P., Murzin A., and Williams R. L. (1997) *Proc. Natl. Acad. Sci. U.S.A. 94*, 9637−9642.
19. Martsev, S. P., Kravchuk, Z. I., Chumanevich, A. A., Vlasov, A. P., Dubnovitsky, A. T., Bespalov I. A., Arosio, P., and Deyev, S. M. (1998) *FEBS Lett. 441*, 458−462.
20. Martsev, S. P., Preygerzon, V. A., Mel'nikova, Ya. I., Kravchuk, Z. I., Ponomarev, G. V., Lunev V. E., and Savitsky, A. P. (1995) *J. Immunol. Methods 186*, 293−304.
21. Kravchuk, Z. I., Chumanevich, A. A., Vlasov, A. P., and Martsev, S. P. (1998) *J. Immunol. Methods 217*, 131−141.
22. Martsev, S. P., Kravchuk, Z. I., Vlasov, A. P., and Lyakhnovich, G. V. (1995) *FEBS Lett. 361*, 173−175.
23. McKiney, M. M., and Parkinson, A. (1987) *J. Immunol. Methods 96*, 271−275.
24. Martsev, S. P., Vlasov, A. P., and Arosio. P. (1998) *Protein Eng. 11*, 377−381.
25. Privalov, P. L., and Khechinashvili, N. N. (1974) *J. Mol. Biol. 86*, 665−684.
26. Privalov, P. L., and Potekhin, S. A. (1986) *Methods Enzymol. 131*, 4−51.
27. Makhatadze, G. I., and Privalov, P. L. (1990) *J. Mol. Biol. 213*, 375−384.
28. Thannhauser, T. W., Konishi, Y., and Scheraga, H. (1984) *Anal. Biochem. 138*, 181−188.
29. Ellman, G. L. (1959) *Arch. Biochem. Biophys. 82*, 70−77.
30. Laemmli, U. K. (1970) *Nature 227*, 680−685.
31. Gill, S. C., and von Hippel, P. H. (1989) *Anal. Biochem. 182*, 319−326.
32. Sun, M., Li, L., Gao, Q. S., and Paul, S. (1994) *J. Biol. Chem. 269*, 734−738.
33. Schodin, B., and Kranz, D. M. (1993) *J. Biol. Chem. 268*, 25722−25727.
34. Kipriyanov, S. M., Dubel, S., Breitling, F., Kontermann, R. E., and Little, M. (1994) *Mol. Immunol. 31*, 1047−1058.
35. Deonarain, M. P., Rowlinson-Busza, G., George, A. J. T., and Epenetos, A. (1997) *Protein Eng. 10*, 89−98.
36. Ward, E. S., Gussow, D., Griffiths, A. D., Jones, P. T., and Winter, G. (1989) *Nature 341*, 544−546.
37. Davies, J., and Riechmann, L. (1996) *Protein Eng. 9*, 531−537.
38. Buchner, J., Renner, M., Lilie, H., Hinz, H.-J., Jaenicke, R., Kiefhaber, T., and Rudolf, R. (1991) *Biochemistry 30*, 6922−6929.
39. Lilie, H., and Buchner, J. (1995) *FEBS Lett. 362*, 43−46.
40. Tsunenaga, M., Goto, Y., Kawata Y., and Hamaguchi, K. (1987) *Biochemistry 26*, 6044−6051.
41. Semisotnov, G. V., Rodionova, N. A., Razgulyaev, O. I., Uverski, V. N., Gripas, A. F., and Gilmanshin, R. I. (1991) *Biopolymers 31*, 119−128.
42. Engelhard, M., and Evans, P. A. (1995) *Protein Sci. 4*, 1553−1562.
43. Privalov, P. L. (1982) *Adv. Protein Chem. 35*, 1−104.
44. Manly, S. P., Matthews, K. S., and Sturtevant, J. M. (1985) *Biochemistry 24*, 3842−3846.
45. Hu, C. Q., and Sturtevant, J. M. (1987) *Biochemistry 26*, 178−182.
46. Brandts, J. F., Hu, C. Q., Lin, L. N., and Mas, M. T. (1989) *Biochemistry 28*, 8588−8596.
47. Hagihara Y., and Goto, Yu. (1998) in *Molecular chaperones in the life cycle of proteins* (Fink, A. L., and Goto, Yu., Eds.) pp 1−33, Marcel Dekker, Inc., Basel, New York, and Hong Kong.
48. Buchner, J., and Rudolph, R. (1991) *Bio/Technology 9*, 157−162.
49. Buchner, J., Pastan, I., and Brinkman, U. (1992) *Anal. Biochem. 205*, 263−270.
50. Buchner, J., Brinkmann, U., and Pastan, I. (1992) *Bio/Technology 10*, 682−685.
51. Pfeil, W., Notlig, B. O., and Jung, C. (1993) *Biochemistry 32*, 8856−8862.
52. Shortle, D., and Meeker, A. K. (1989) *Biochemistry 28*, 936−944.
53. Shortle, D. (1996) *FASEB J. 10*, 27−34.
54. Reddy, G. B., Srinivas, V. R., Ahmad, N., and Surolia, A. (1999) *J. Biol. Chem. 274*, 4500−4503.
55. Bose, H. S., Whittal, R. M., Baldwin, M. A., and Miller, W. L. (1999) *Proc. Natl. Acad. Sci. U.S.A. 96*, 7250−7255.
56. Jiang, J. X., and London, E. (1990) *J. Biol. Chem. 265*, 8638−8641.
57. Huber, R. (1979) *Cell. Ges. Biol. Chem. 30*, 1−16.
58. Jaenicke, R. (1987) *Prog. Biophys. Mol. Biol. 49*, 117−237.
59. Williams, R. P. J. (1989) *Eur. J. Biochem. 183*, 479−497.
60. Shoichet, B. K., Baase, W. A., Kuroki, R., and Matthews, B. W. (1995) *Proc. Natl. Acad. Sci. U.S.A. 92*, 452−456.
61. Glockshuber, R., Malia, M., Pfitzinger, I., and Pluckthun, A. (1990) *Biochemistry 29*, 1362−1367.
62. Brinkmann, U., Reiter, Y., Jung, S.-H., Lee, B., and Pastan, I. (1993) *Proc. Natl. Acad. Sci. U.S.A. 90*, 7538−7542.
63. Reiter, Y., Brinkmann, U., Jung, S.-H., Pastan, I., and Lee, B. (1995) *Protein Eng. 8*, 1323−1331.
64. Webber, K. O., Reiter, Y., Brinkmann, U., and Pastan, I. (1995) *Mol. Immunol. 32*, 249−258.
65. Reiter, Y., Brinkmann, U., Lee, B., and Pastan, I. (1996) Engineering antibody Fv fragment for cancer therapy: disulfide-stabilized Fv fragments; *Nat. Biotechnol. 14*, 1239−1245.
66. Rajagopal, V., Pastan., I., and Kreitman, R. (1997) *Protein Eng. 10*, 1453−1459.
67. Reiter, Y., Brinkmann, U., Kreitman, R. J., Jung, S.-H., Lee, B., and Pastan, I. (1994) *Biochemistry 33*, 5451−5459.
68. Reiter, Y., Pai., L. H., Brinkmann, U., Wang, Q. C., and Pastan, I. (1994) *Cancer Res. 15*, 2714−2718.
69. Bera, T. K., Onda, M., Brinkmann, U., and Pastan, I. (1998) *J. Mol. Biol. 281*, 475−483.
70. Worn, A., and Pluckthun, A. (1998) *Biochemistry 37*, 13120−13127.

71. Worn, A., and Pluckthun, A. (1999) *Biochemistry 38*, 8739−8750.
72. Uversky, V. N, Kutyshenko, V. P., Protasova, N. Yu., Rogov, V. V., Vassilenko, K. S., and Gudkov, T. (1996) *Protein Sci. 5*, 1844−1851.
73. Edelman, G. M. (1970) *Biochemistry 9*, 3197−3205.
74. Davies, J., and Riechmann, L. (1995) *Bio/Technology 13*, 475−479.
75. Sheriff, S., and Constantine, K. L. (1996) *Nat. Struct. Biol. 3*, 733−736.
76. Freund, C., Honegger, A., Hunziker, P., Holak, T. A., and Pluckthun, A. (1996) *Biochemistry 35*, 8457−8454.
77. Freund, C., Gehrig, P., Hollak, T. A., and Pluckthun, A. (1997) *Folding Des. 3*, 39−49.
78. Jager, M., and Pluckthun, A. (1997) *FEBS Lett. 418*, 106−110.
79. Jager, M., and Pluckthun, A. (1999) *J. Mol. Biol. 285*, 2005−2019.
80. Nilson, B. (1995) *Curr. Opin. Struct. Biol. 5*, 450−456.

BI992036D